Can Uplift of the Andes Influence the Pacific Meridional Overturning Circulation?

Mingjun Tong[a], Haijun Yang[a*], Fengli An[a], and Peili Wu[b]

[a] *Department of Atmospheric and Oceanic Sciences and Key Laboratory of Polar Atmosphere-ocean-ice System for Weather and Climate of Ministry of Education, Fudan University, Shanghai, 200438, China.*

[b] *Met Office Hadley Centre, Exeter, United Kingdom*

Journal of Climate

1st submission: September 12, 2025

**Corresponding author address*: Haijun Yang, Department of Atmospheric and Oceanic Sciences, Fudan University, 2005 Songhu Road, Shanghai, 200438, China.

Email: yanghj@fudan.edu.cn

Abstract

The uplift of major mountain ranges plays an important role in shaping modern day ocean circulation. From a paleoclimatic perspective, the understanding of how uplift of the Andes influences Earth's climate and the global ocean conveyor is of great interest. Using the topography-sensitive Community Earth System Model 1.0 simulations, it is shown that Andes uplift weakens the equatorial easterlies, triggering a surface warming along the equator and in the eastern Pacific. Ocean circulation adjusts to this warming by an intensification of North Pacific subtropical gyre in the horizontal and a strengthening of the Pacific Meridional Overturning Circulation (PMOC) in the vertical. A stronger subtropic gyre transports more warm water to the subpolar northeast Pacific, where local surface salinification occurs as a result of increased evaporation. This consequently raises surface density and triggers North Pacific deep-water formation. Such a mechanism suggests that a vigorous PMOC can emerge without elevated CO_2 concentrations or open tropical seaways, offering new insights into the tectonic regulation of past ocean circulation.

Keywords: Andes uplift, Pacific Meridional Overturning Circulation, topographic forcing, paleoclimate, CESM

Plain Language Summary

The rapid uplift of the Andes began in the late Miocene (10–6 Ma), coinciding with an active PMOC in the warm Pliocene (5.3–2.6 Ma) — a link of great interest to paleoclimate scientists. Our simulations show that Andes uplift not only induces local cooling in the tropical southeastern Pacific but also remotely enhances the PMOC. The latter occurs through the acceleration of the subtropical gyre, the Kuroshio Current, and its extension, which increases surface salinity and thus density in the subpolar northeast Pacific, facilitating the formation of the PMOC, a Pacific counterpart to the well-known Atlantic Meridional Overturning Circulation (AMOC). Understanding these processes provides insights into how ocean circulation might respond to future environmental changes.

1. Introduction

The global meridional overturning circulation (GMOC) acts as a conveyor belt, transporting energy and freshwater between hemispheres (Rahmstorf 2002). Today, the Atlantic Meridional Overturning Circulation (AMOC) dominates global ocean conveyor belt, while the Pacific hosts only a shallow wind-driven cell. Strong deep-water formation in the North Atlantic, reinforced by Ekman pumping in the Southern Ocean, sustains the modern AMOC. This circulation pattern helps maintain colder climates in northwestern North America and warmer conditions in Northwestern Europe (Saenko et al. 2004).

Paleoclimate studies suggest that an active Pacific Meridional Overturning Circulation (PMOC) may have existed during mid-Pliocene, derived from isotopic evidence that support a strong deep-water formation in the North Pacific (Burls et al. 2017; Fu and Fedorov 2024). The Pliocene, characterized by CO_2 levels near 400 ppm, represents a climate state comparable to future warming scenarios, during which the AMOC and PMOC could coexist. However, state-of-the-art models from the Paleoclimate Modelling Intercomparison Project Phase 4 (PMIP4) – Coupled Model Intercomparison Project Phase 6 (CMIP6) are only capable of simulating a strong AMOC, while failing to produce deep water formation in the North Pacific. A strong PMOC can only be reproduced in some sensitivity experiments, including the application of negative freshwater forcing in the North Pacific (Fu and Fedorov 2024), positive freshwater perturbations in the North Atlantic (Okazaki et al. 2010), and modifications to cloud radiative forcing (Burls et al. 2017), among others. A Pliocene-like simulation identified a key difference: while most PMOC water upwells in the Southern Ocean, they also form stronger connections with the tropical ocean, a feature weaker in the AMOC (Thomas et al. 2021). Despite of studies supporting an active PMOC in the Pliocene, Novak et al. (2024) argues that it is unlikely that North Pacific Deep Water (NPDW) formation occurred in the mid-Piacenzian warm period (late Pliocene). Based on abundant isotopic data located around 50°N, they speculate that bottom-up ventilation, rather than a deep-reaching PMOC, occurred in the subpolar North Pacific during the late Pliocene—an aspect that has been largely overlooked in previous studies.

Some studies also suggest that the shallow openings of the Panamanian and Indonesian seaways might influence NPDW formation from the late Miocene to the Pliocene, though the underlying mechanisms varied with continental boundary conditions (Motoi et al. 2005; Tan et al. 2022). Besides, evidence indicates that the PMOC was active during the last glacial maximum (LGM) and last deglaciation termination (17.5–15 kyr ago) (Okazaki et al. 2010; Rae et al. 2020), when tropical

seaways were already closed. The Indonesian seaway was closed between 3–4 Ma, while the final closure of the Central American seaway occurred between 3.7–3 Ma, predating the LGM. At the onset of deglaciation, the AMOC collapsed into a weak state in response to high-latitude glacial melt, nearly coinciding with PMOC activation (Bond et al. 1992). The enhanced PMOC during the LGM likely contributed to Beringia warming, potentially facilitating human migration from Asia to North America (Rae et al. 2020). These findings suggest that the openings of tropical seaways were not the primary drivers of PMOC formation. Moreover, since the PMOC was active during both colder climate (such as the LGM) and warmer climate (like the mid-Pliocene), it also suggests that temperature may not the controlling factor.

A recent modeling study on GMOC evolution since the Paleozoic found that continental configuration plays a more crucial role than climate evolution in shaping ocean circulation (Yuan et al. 2024). In the early Paleozoic, most continents were in the Southern Hemisphere, driving a counterclockwise GMOC. Studies on global topography suggest that mountain uplift enhances AMOC strength (Schmitter et al. 2012; Maffre et al. 2018; Su et al. 2018). Among key mountain ranges, the Tibetan Plateau (TP) plays a vital role in regulating both the AMOC and PMOC (Yang et al. 2024). Additionally, topographic experiments indicate that Antarctic uplift-induced Ekman upwelling is also essential for fully establishing a strong AMOC (Tong et al. 2025). Compared to the AMOC, research on the impact of land topography on the PMOC is limited, as the modern Pacific only supports a shallow overturning cell.

This study aims to investigate exclusively the teleconnection between the uplift of Andes Mountains (AM) and the development of PMOC. The rapid AM uplift during the mid- to late-Miocene (Isacks 1988; Lamb and Davis, 2003) may have connection with later strong NPDW formation and thus the PMOC establishment in the warm Pliocene. However, most studies on AM uplift focus on regional effects. Insel et al. (2010) showed that Andes topography significantly alters moisture transport and deep convection between the Amazon Basin and central Andes. Xu and Lee (2021) linked AM uplift to sea surface temperature (SST) cooling in the southeastern Pacific. Several studies attribute this to increased surface evaporation, enhanced low-level cloud cover, and a strengthened Walker Circulation, forming a cold tongue in the tropical southeastern Pacific (Xu et al. 2004; Sepulchre et al. 2009; Feng and Poulsen 2014). Despite these findings, limited attention has been given to the remote effects of AM uplift. Since strong warming signals in the North Pacific

associated with AM uplift have also been identified in previous studies (Xu and Lee 2021; Feng and Poulsen 2014), AM uplift may have potential impacts on NPDW formation.

This paper is organized as follows. In section 2, model and experiments used in this study are introduced. In section 3, we briefly analyze the regional impacts of AM uplift. In section 4, the remote effects of AM uplift are examined, focusing mainly on how ocean circulations in the North Pacific response to the AM uplift and the underlying mechanisms. A summary of our findings is presented in section 5, together with a discussion on their implications.

2. Model and Experiments

In this study, we conducted topography-sensitive experiments using the Community Earth System Model (CESM) version 1.0.4. Developed by the U.S. National Center for Atmospheric Research (NCAR) in collaboration with the climate research community, CESM is a fully coupled model widely used for simulating climate in the past, present and future. To optimize computational resources for long-term simulations, we employed a coarse resolution (T31_gx3v7). The atmospheric and land components have a 3.75° × 3.75° horizontal resolution with 26 vertical levels, while the ocean model features a variable horizontal resolution (~0.6° near the equator, 3.4° in midlatitudes) with 60 vertical layers. More details on CESM1.0 can be found in Hurrell et al. (2013). The model configuration and boundary conditions used in this study align with the preindustrial period, where atmospheric CO_2 concentration was 285 ppm.

To investigate the impacts of AM uplift on the PMOC, we build upon the experiments of Yang et al. (2024) and extend their integration period. We mainly analyze two experiments in detailed in this work: Flat and OnlyAndes experiments (Fig. 1). In Flat, all major mountain ranges are removed, with global elevations set to 10 meters above sea level. In OnlyAndes, the AM are restored to its original altitude, while all other topography remains flattened. Both experiments run for more than 3000 years, aiming to isolate the role of AM without interference from other major topographies. A realistic topography experiment (Real) from Yang et al. (2024) is included for comparison. Our earlier studies have deliberated why the PMOC is absent in the modern climate despite the presence of the AM, and how the modern AMOC was established through the sequential uplift of major mountain ranges (Yang et al. 2024). Here, we specifically examine how the AM uplift alone promotes the PMOC development, using the Flat and OnlyAndes experiments.

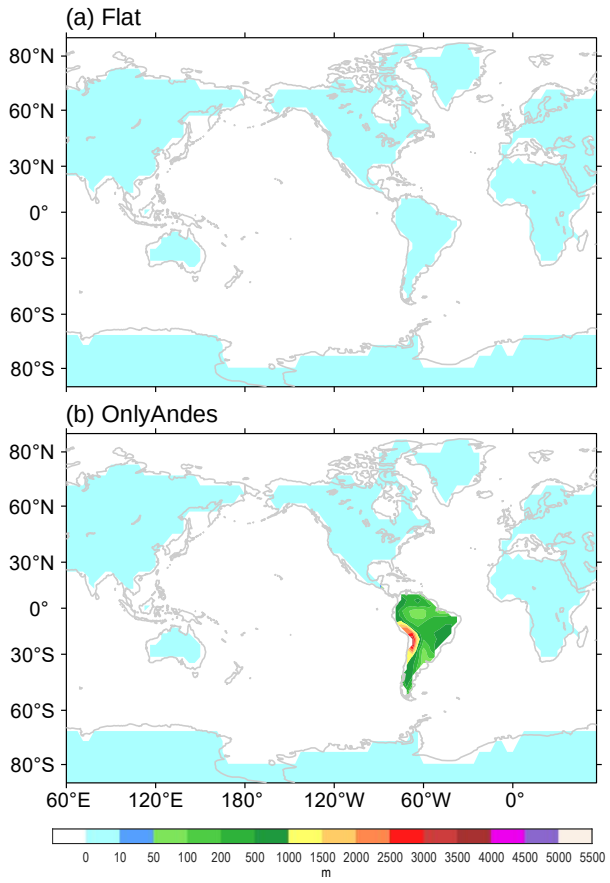

FIG.1. Topography configuration in coupled model experiments. (a) Modified topography with flat global topography used in Flat, (b) modified topography with the inclusion of the Andes Mountains used in OnlyAndes, Shading represents surface geopotential heights (m).

In all topographic sensitivity experiments, only the elevations of specific mountain ranges are altered; river routing and vegetation types remain unchanged. Continental ice sheets are represented as inert “bright rocks,” allowing planetary albedo to adjust dynamically to thermal conditions. Unless otherwise specified, annual mean model outputs are used for analysis. Climate responses to AM uplift are defined as the difference between the OnlyAndes and Flat experiments. Quasi-equilibrium responses are obtained by averaging these differences over the final 600 years. Statistical significance is assessed using the Student’s t-test, with most changes found to be significant at the 95% confidence level. For visual clarity, significance markers are not shown in the figures.

3. Regional impacts of AM uplift

Acting as a mechanic barrier, the uplifted north-south-oriented AM deflects equatorial easterlies and obstructs subtropical westerlies in the Southern Hemisphere, inducing subsidence along its western slopes and ascent on the eastern side. Figure 2a shows that topographic forcing generates a cyclonic anomalous wind to the west of the AM, characterized by westerly anomalies on and north of the equator, which are also found in previous studies (Xu and Lee 2021; Xu et al. 2004; Feng and Poulsen 2014; Sepulchre et al. 2009). At the same time, a notable surface cooling emerges in the tropical southeastern Pacific (Fig. 2a). Three primary processes contribute to this cooling: (1) Radiative cooling – AM uplift increases low-level marine boundary layer clouds (Bony 2005; Fig. 2b), enhancing shortwave cloud forcing and reinforcing the cold tongue in the tropical southeastern Pacific. (2) Evaporative cooling – By blocking midlatitude westerlies, the AM deflect surface winds equatorward (Fig. 2a). Strengthened northwestward surface winds enhance net evaporation (Fig. 2c) and latent heat flux (figure not shown). The increased evaporation also causes higher sea surface salinity (SSS) (Fig. 2d). (3) Ekman pumping cooling – Intensified northwestward winds strengthen Ekman pumping near the western coast of South America (Fig. 2e), further promoting cooling. These local responses are also consistent with earlier findings using simplified atmospheric general circulation model (GCM) coupled to an idealized ocean model (Takahashi and Battisti 2007), which emphasize the mechanical role of AM in driving air subsidence and sustaining evaporative cooling in this region.

Apart from the cooling signal south of the equator, slight surface warming emerges on the equator (Fig. 2a). The weakened the trade winds (Fig. 2a) lead to eastward return of warm water from the western Pacific warm pool. Reduced net evaporation (Fig. 2c) and decreased low cloud over the equator (Fig. 2b) also contribute to the equatorial surface warming. The warming pattern in the eastern equatorial Pacific resembles the tropical SST pattern in mid-Pliocene (Dekens at al. 2008; Dowsett et al. 2009). Overall, the equatorial SST becomes slightly more zonally homogenized in response to the AM uplift.

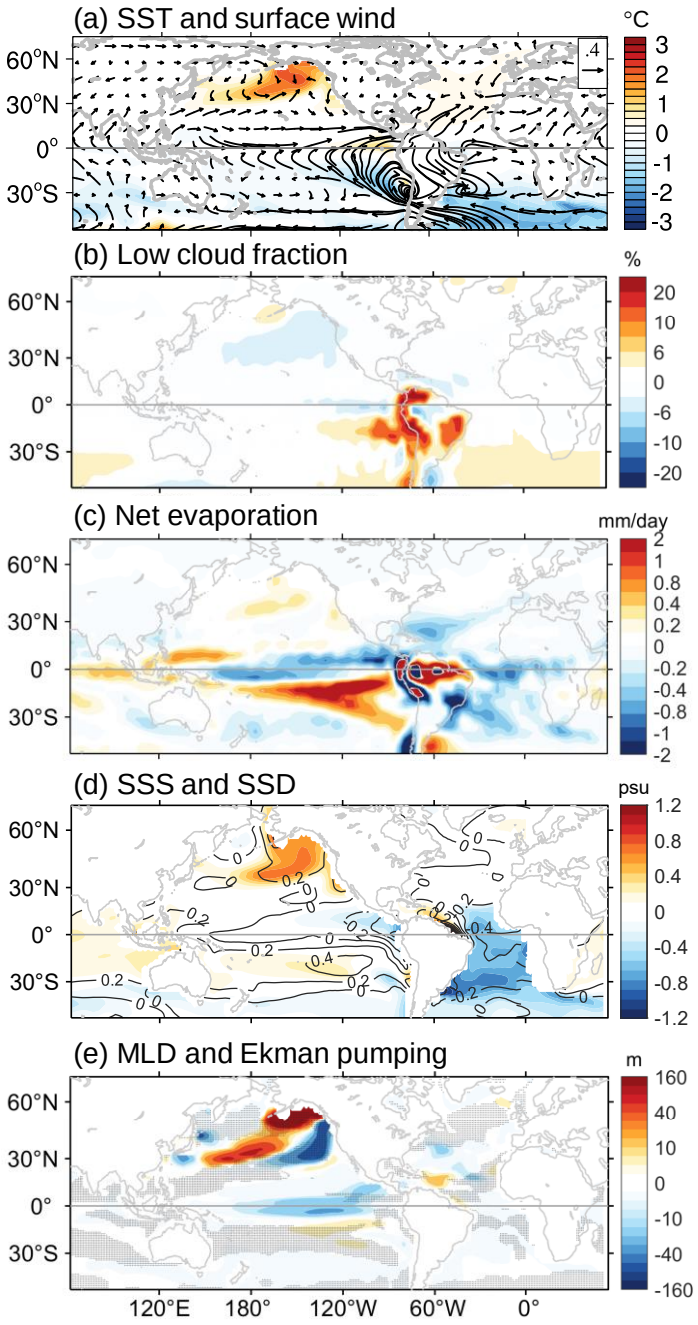

FIG.2. Equilibrium climate response to the AM uplift. (a) Changes in sea surface temperature (SST, shading; units: °C) and winds (arrows; units: m/s), (b) Low cloud change (units: %), (c) Net evaporation change (i.e., evaporation minus precipitation, EMP; units: mm/day), (d) Changes in sea surface salinity (SSS, shading; units: psu) and sea surface density (SSD, contours; units: kg/m^3) and (e) Changes in March mixed layer depth (MLD, shading; units: m) and Ekman pumping (stripped area represents Ekman downwelling). Note that Ekman pumping within 2°S-2°N is not calculated.

4. Remote responses and the PMOC

The remote response in the extratropical North Pacific is a central focus of this study, where pronounced surface warming, salinification, and deepening of mixed layer depth (MLD) occur (Figs 2a, d, e). These changes enhance North Pacific ventilation and facilitate the development of the PMOC. While similar SST warming has been reported in Richter et al. (2022), the accompanying salinity changes have received less attention. Our experiments demonstrate that robust NPDW formation can be triggered solely by AM uplift—without requiring extreme warming (e.g., 400-ppm CO_2 during the Pliocene), Bering Strait closure (as during the LGM), or AMOC shutdown via freshwater forcing. This study seeks to elucidate the mechanisms behind these remote responses: how AM uplift drives warming and salinification in the subpolar Pacific, and how these changes promote NPDW formation.

In our experiments, the PMOC strength in Flat is approximately 10 Sv (Fig. 3a), with its lower branch reaching depths of around 1000 m (Fig. 3b). This pattern contrasts markedly with the realistic topography case (Real), where the PMOC is largely absent (Fig. 3d). When the AM is uplifted, the PMOC intensifies by approximately 50% to ~15 Sv and penetrates deeper, to about 2000 m (Fig. 3c), whereas the AMOC remains largely inactive (Fig. 3f). In Flat, the AMOC is extremely weak (Fig. 3e), in sharp contrast to its robust strength under modern topography (Fig. 3g). Other studies have also identified the activation of a PMOC in flattened topography. For instance, simulations using the Institut Pierre-Simon Laplace (IPSL) model reveal a shift in deep convection from the North Atlantic to the Gulf of Alaska under flattened conditions (Maffre et al. 2018). Similar Atlantic-to-Pacific shifts in deep convection have been reported in the mountain-free experiments of Schmittner et al. (2011) and Sinha et al. (2012). The mechanisms underlying this meridional overturning circulation "see-saw"—from the Atlantic in Real to the Pacific in Flat—have been thoroughly investigated in these earlier works.

It is worth noting that PMIP4 control simulations for the mid-Pliocene fail to reproduce a strong PMOC (Fu and Fedorov 2024). To address this limitation, several modeling studies have conducted sensitivity experiments to artificially activate the PMOC—for example, by applying negative freshwater forcing in the subpolar North Pacific (Fu and Fedorov 2024) or modifying cloud radiative forcing to reduce meridional SST gradients (Burls et al. 2017). However, unlike the North Atlantic, the subpolar North Pacific is not directly connected to the Arctic Ocean, making freshwater perturbations there less physically plausible as a mechanism for triggering deep-water formation. In

contrast, our topography experiments suggest that the AM uplift may have been a key factor in strengthening the PMOC during the mid-Pliocene.

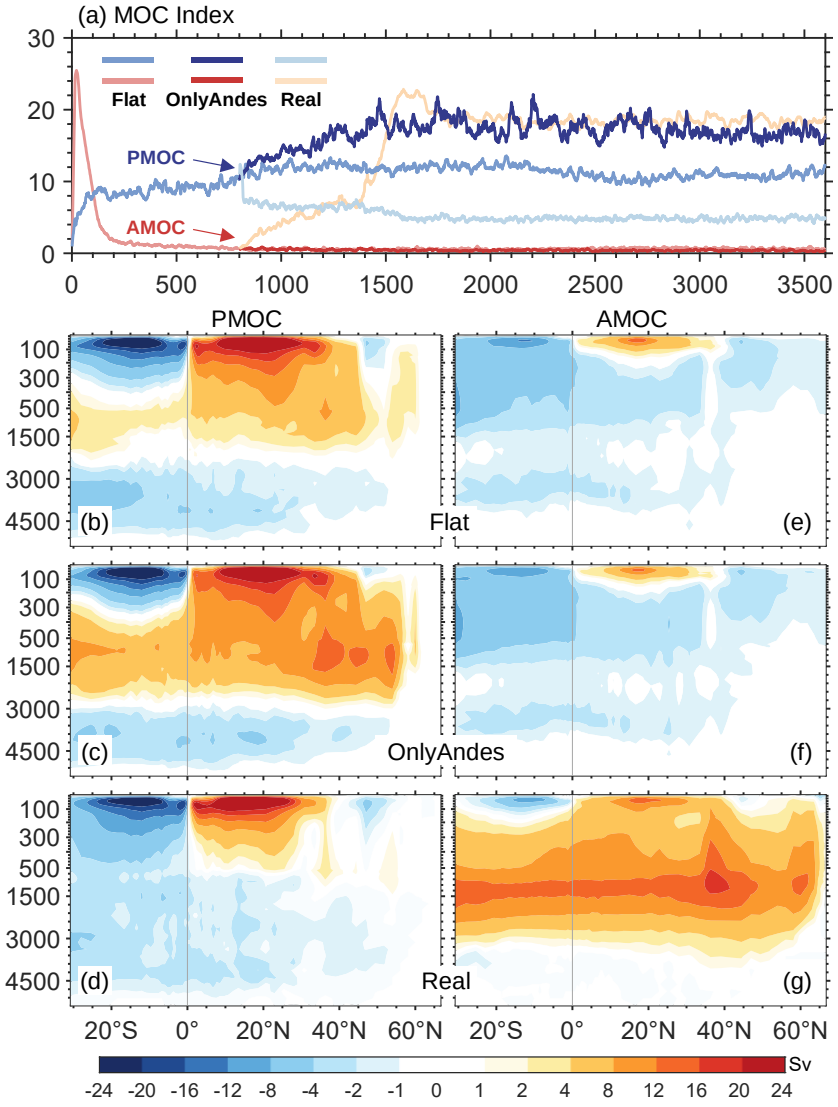

FIG. 3. Meridional overturning circulations and their changes in different experiments. (a) Temporal evolution of the Pacific Meridional Overturning Circulation (PMOC, blue curves) and Atlantic Meridional Overturning Circulation (AMOC, red curves) in topography experiments (units: Sv; 1 Sv = 10^6 m^3 s^{-1}). The AMOC index is defined as the maximum stream function at depths of 400–2000 m in the North Atlantic, while the PMOC index is calculated similarly for the North Pacific. All curves are smoothed using a 15-year running mean. (b–d) Zonally averaged streamfunction of the PMOC in the (b) Flat, (c) OnlyAndes, and (d) Real experiments. (e–g) AMOC streamfunction patterns for the same experiments. All patterns are averaged over the last 600 years.

a. Oceanic process dominates PMOC enhancement

The development of the PMOC results from the slow oceanic adjustment in response to the AM uplift. To trace this evolution, we analyze situation in the subpolar northeast Pacific region (40°N–60°N, 180°E–120°W). Gradual increases in SST, SSS, and March MLD (Fig. 4a) suggest that their changes are not driven by transient atmospheric processes. This is further supported by the evolution of latent heat flux and evaporation (Fig. 4b, c), which show similar trends. In contrast, net surface shortwave, longwave and sensible heat flux (Fig. 4b) do not exhibit such clearly progressive changes. Moreover, the positive net surface flux (i.e., the heat loss from ocean to atmosphere by definition; Fig. 4b) confirms that the surface ocean warming results from ocean dynamics rather than atmospheric processes. In general, the evolution timescales of SST, SSS, MLD, evaporation and latent heat flux align well with the PMOC intensification (Fig. 3a), which occurs over approximately 600 years (model year 801 to 1400). These concurrent changes support the view that oceanic processes play the dominant role in the PMOC response.

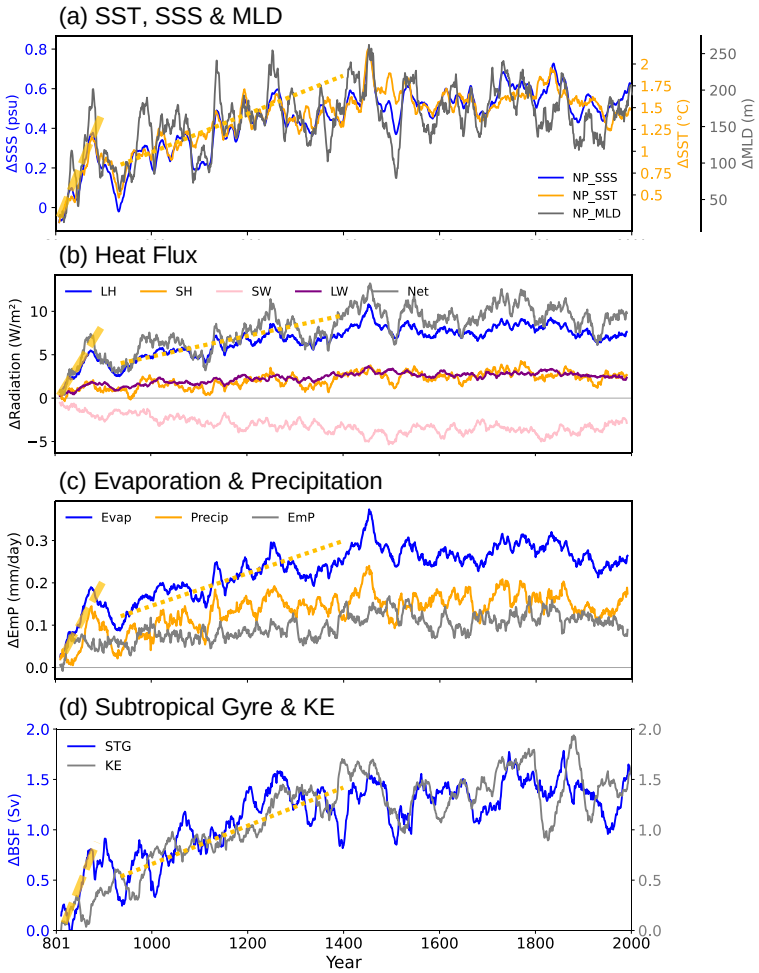

FIG.4. Temporal evolution of area averaged ocean and surface flux variables over the subpolar Pacific (40°E–60°N, 180°–120°W) in response to the AM uplift. (a) Changes in SST (orange; units: C), SSS (blue; units: psu) and March MLD (grey; units: m). (b) Changes in surface heat flux components (units: W/m^2). Positive value denotes upward flux from ocean to atmosphere, i.e., ocean loses heat to atmosphere. Pink for net surface shortwave radiation, dark red for net surface longwave radiation, orange for sensible heat flux, blue for latent heat flux and grey for net surface flux. (c) Changes in surface freshwater flux (units: mm/day). Blue for ocean surface evaporation (positive value denotes that ocean loses freshwater to atmosphere), orange for ocean surface precipitation (positive value denotes that ocean gains freshwater) and grey for EMP. (d) Changes in the strength of subtropical gyre (blue) and Kuroshio Extension (grey) (units: Sv), which are defined as area-averaged streamfunction over the regions of 20°–35°N, 120°–140°E and 45°-48°N, 140°-160°E, respectively. Thick and thins dashed orange lines mark trend in the first 100 years and the following 500 years, respectively.

The ocean evolution appears to unfold in two distinct phases: an initial rapid adjustment during the first ~100 years, followed by a slower, quasi-linear progression. These two phases are marked by thick and thin dashed orange lines in Fig. 4. Based on these trends, we propose the following mechanism for PMOC enhancement: subpolar Pacific surface warming → enhanced evaporation and increased latent heat loss → surface salinification → denser surface waters → activation of NPDW formation → strengthened PMOC. However, a key question remains: what causes SST to rise in the subpolar northeast Pacific in response to the AM uplift?

Let us focus on the rapid adjustment during the first 100 years. In response to the sudden AM uplift, westward-propagating Rossby waves play a critical role in intensifying the subtropical gyre and the Kuroshio current (Fig. 4d), thereby initiating a chain reaction that ultimately enhances the PMOC. During the first several decades, the SST exhibits slight warming along the equator (Fig. 5a), triggered by weakened easterlies (Fig. 5b). The spatial patterns of equatorial SST and wind anomalies already resemble those in the final equilibrium state (Fig. 2a). This equatorial warming leads to sea level rise, especially in the eastern equatorial Pacific (Fig. 5b), which can be interpreted as a fast Kelvin wave response propagating eastward along the equator. Upon reaching the eastern boundary of the Pacific, the signal deflects poleward along the American coasts and subsequently generates westward-propagating Rossby waves. The pattern of sea surface height (SSH) anomaly (Fig. 5b) clearly exhibits these Rossby wave signatures in the Pacific north of 15°N.

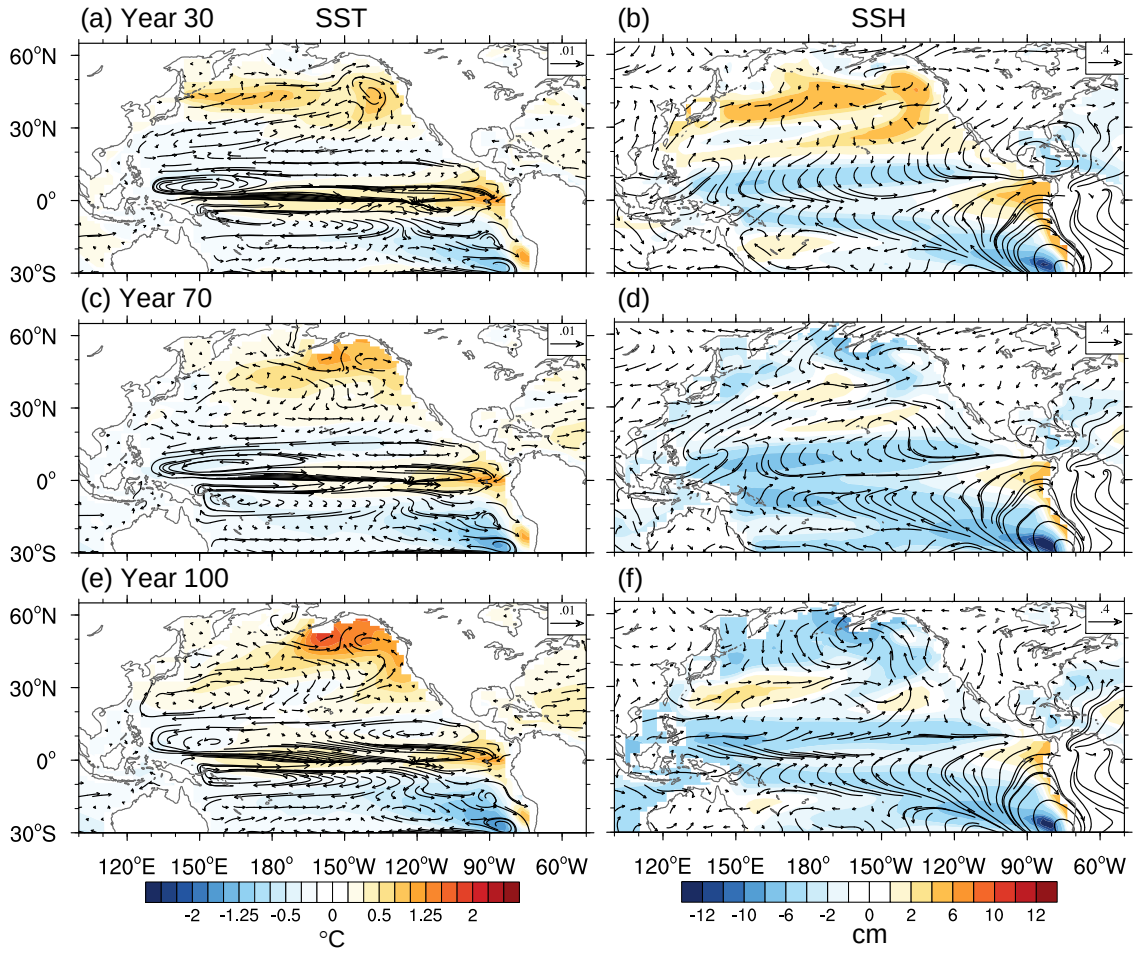

274

275 FIG. 5. Transient changes in SST, upper ocean circulation, SSH and surface winds in response to the AM
276 uplift. (a) Changes in SST (shading; units: °C) and upper 0-100 m averaged ocean circulation (vector; units:
277 m/s; reference vector: 0.01 m/s) in the first 30 years (averaged over years 5-30). (b) Changes in sea surface
278 height (SSH, shading; units: cm) and surface winds (vectors; units: m/s; reference vector: 0.4 m/s) in the first
279 30 years. (c)-(d) and (e)-(f) are same as (a)-(b), but for changes averaged over years 31-70 and 71-100,
280 respectively.

281

282 In about 70 years after the AM uplift, the SSH anomaly pattern indicates that the westward-
283 propagating Rossby waves have largely completed their adjustment (Fig. 5d), particularly in the
284 tropical-subtropical North Pacific. Concurrently, SST anomalies show a clearly eastward extension of
285 warming into the subpolar northeastern Pacific (Fig. 5c). This suggests that warm waters, initially
286 occurs along the latitude band of 40°-50°N (Fig. 5a), are carried by the enhanced Kuroshio Extension
287 and gradually reach the subpolar regions.

In about 100 years, the wave dynamics complete their role—strengthening the subtropical gyre and Kuroshio Extension (Fig. 5e), which enhances the advection of warm water into the subpolar North Pacific. During this period, both surface ocean circulation and winds reach quasi-equilibrium (Figs. 5e–f). The resulting SSH anomaly pattern (Fig. 5f) differs significantly from the initial state (Fig. 5b) and aligns with the enhanced subtropical gyre and subpolar cyclonic wind anomalies: the positive SSH anomaly in the subtropic reflects the intensified subtropical gyre, while the negative anomaly in the subpolar Pacific corresponds to cyclonic circulation. Notably, the surface warming in the subpolar Pacific (Fig. 5e) is primarily due to the enhanced warm water advection via the intensified subtropical gyre and Kuroshio Extension, rather than local surface wind or SSH changes. Changes in surface heat fluxes further support this, as only the latent heat flux follows the SST trend (Fig. 4b), and it reflects, rather than causes, the SST increase.

Figure 6 presents Hovmöller diagrams of SSH, SST, and SSS anomalies following the AM uplift. In the subtropical Pacific, SSH anomalies exhibit clear westward propagation (Fig. 6a), consistent with Rossby wave dynamics. Correspondingly, SST anomalies in the subpolar Pacific display eastward advection (Fig. 6b), reflecting enhanced warm water transport by the Kuroshio current and its extension from the subtropics. In contrast, SSS anomalies in the subpolar Pacific develop locally in the east, showing no clear horizontal propagation (Fig. 6c). This supports our earlier inference that surface salinification results from in situ processes, particularly enhanced evaporation driven by surface warming (Fig. 4c).

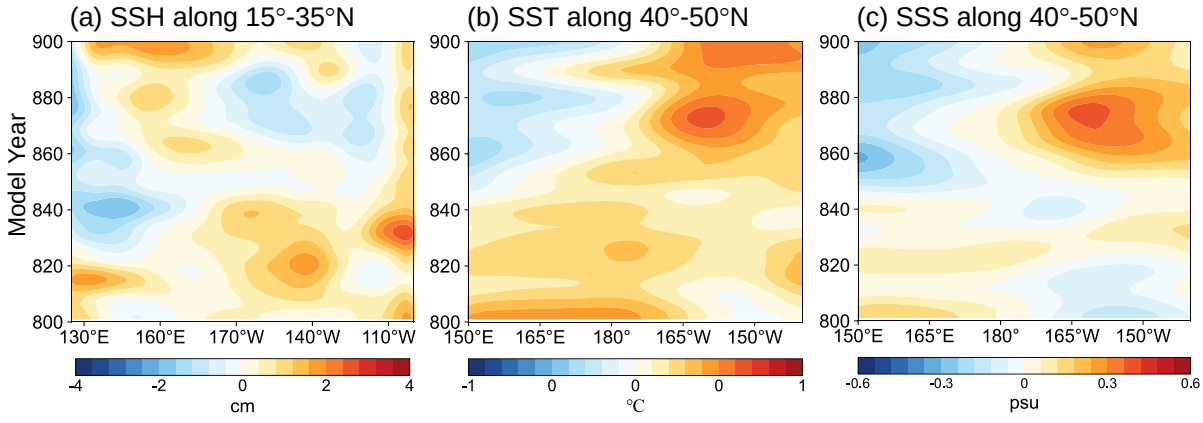

FIG.6. Hovmöller diagrams of SSH, SST and SSS changes in response to the AM uplift. (a) SSH anomaly (units: cm) averaged over latitudes 15°-35°N. (b) and (c) are for SST (units: °C) and SSS (units: psu) anomalies averaged over latitudes 40°-50°N, respectively.

Here we would like to explain the early-stage SST warming observed in the subpolar Pacific in Fig. 5a. This warming is closely associated with meridional atmospheric circulation adjustments triggered by the AM uplift. As illustrated in Fig. 7a, the northern branch of the Hadley cell shifts southward in the decades following the uplift, accompanied by a concurrent southward shift of the Ferrel cell. These changes result in anomalous northward low-level mass transport in the subtropical to subpolar regions of the Northern Hemisphere. This anomalous meridional circulation also enhances northward low-level atmospheric heat transport (indicated by dashed orange arrows), delivering additional heat to the subpolar Pacific and leading to localized SST warming around 40°–50°N. The southward shift of the northern branch of the Hadley cell is driven by equatorial warming and accompanied weak cooling in the off-equator (Fig. 5a). This altered meridional temperature gradient strengthens the annual mean Hadley circulation in the deep tropics (0°–15°N), enhancing its intensity by up to 20% (Fig. 7a). In summary, the coupling between atmospheric dynamics and ocean surface temperature during this early adjustment phase highlights the critical role of transient atmospheric responses in initiating the development of PMOC-related oceanic processes.

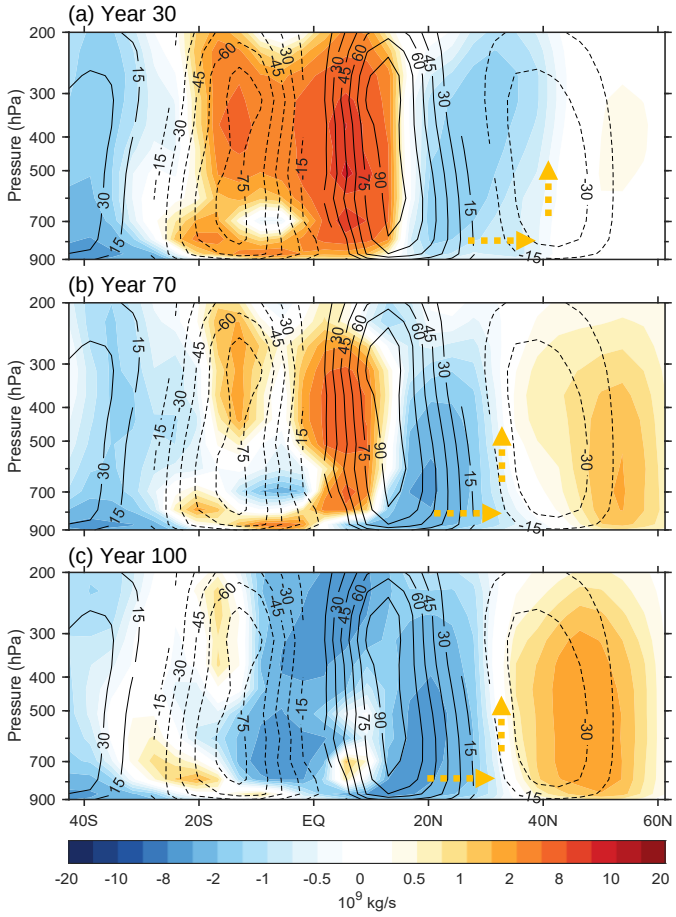

FIG. 7. Transient changes in Hadley circulation in response to the AM uplift. (a) Changes in annual mean Hadley cell (shading; units: 10^9 kg/s) in the first 30 years (averaged over years 5-30). The climatological annual mean Hadley cell in Flat is plotted as black contours. (b), (c) are same as (a), but for changes averaged over years 31-70 and 71-100, respectively. Dashed orange arrows shows anomalous meridional and vertical mass transports in the subtropics.

In the later stages of the simulation, the sustained SST warming in the subpolar Pacific is primarily driven by oceanic processes, as discussed before. As this warming intensifies, the meridional SST gradient between the tropics and high latitudes weakens. This reduction in thermal contrast diminishes the driving force behind large-scale atmospheric circulation, ultimately leading to the weakening of both the Hadley and Ferrel cells, as well as the gradual retreat of the anomalous northward low-level atmosphere heat transport (indicated by dashed orange arrows) (Figs. 7b, c).

b. Subduction in the northern subpolar Pacific

The NPDW is initiated by denser surface waters in the subpolar North Pacific, primarily driven by surface salinification rather than surface warming. Figure 8a presents zonal sections of salinity and density changes along 40°–50°N — latitudes corresponding to the Kuroshio Extension and the North Pacific Current — overlaid with climatological isopycnals. It is clear that the high-salinity, dense surface water is not advected from the western Pacific but instead develops locally in the central-eastern Pacific (160°W–120°W). This saline water mass subducts and penetrates to depths exceeding 2000 m in the subpolar eastern Pacific between 50°–60°N (Fig. 8b). This subduction is further aided by anomalous Ekman downwelling (Fig. 2e). We would like to emphasize that, unlike deep-water formation in the North Atlantic (where high surface density alone is sufficient to sustain deep-water formation), wind-driven downward forcing is crucial for the NPDW (Wen and Yang 2020), because warmer surface waters in the North Pacific limit surface density increases. In addition, we also notice that this deep-water formation appears to be diapycnal, potentially explaining why the PMOC requires nearly 600 years to become fully established.

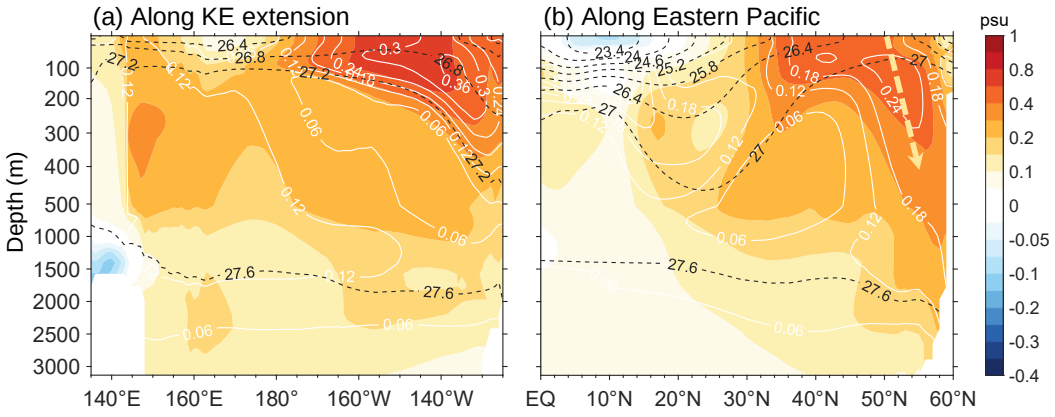

FIG.8. Equilibrium changes in ocean salinity and density in response to the AM uplift. (a) Zonal-depth section of salinity (shading; units: psu) and density (white contours; units: kg/m^3) changes along the Kuroshio extension latitudes (40°-50°N). (b) Same as (a), but for meridional-depth section along Eastern Pacific longitudes (170°E-120°W). The mean isopycnals are plotted as dashed black contours (units: kg/m^3). In (b), the dashed orange arrow illustrates the diapycnal subduction process.

5. Conclusion and discussion

The motivation of this work comes from the historical period of the AM uplift aligns precisely with the active phase of the PMOC during the late Miocene as a result of the subduction of the Nazca Plate beneath South America (Isacks 1988). The final stage of the AM uplift, known as the Diaguita phase, ended around 3 Ma during the Pliocene (Ortiz-Jaureguizar and Cladera 2006), when the summits reached their current height (Renny et al. 2022). Prior studies have reached a consensus that the AM uplift can regulate the regional climate, while the far-reaching impacts remains unrevealed.

In this study, we explored the role of AM uplift in driving changes to Pacific Ocean circulation, particularly the development of the PMOC. Using topography-sensitive simulations with CESM1.0, we find that the AM — by altering atmospheric circulation — trigger a series of remote oceanic responses that lead to the activation of NPDW formation and the development of a robust PMOC. The mechanisms identified can be summarized as follows: (1) Atmospheric Process: AM uplift weakens both the equatorial easterlies and southern subtropical westerlies, which modify the regional SST and SSS distribution. (2) Wave-Driven Adjustment: The weakened easterlies induce equatorial warming, initiating a fast Kelvin wave–Rossby wave response. Westward-propagating Rossby waves intensify the North Pacific subtropical gyre and Kuroshio Extension, promoting warm water transport

eastward and poleward. (3) Local Surface Forcing and Deep-Water Formation: In situ surface warming and enhanced evaporation in the subpolar northeast Pacific increase surface salinity and density, leading to the formation of dense water masses that eventually ventilate the deep Pacific. This deep-water formation is notably diapycnal, contributing to the relatively long (~600 years) adjustment timescale of the PMOC.

Our findings provide new insight into how tectonic processes, particularly the AM uplift, may have contributed to large-scale ocean circulation restructuring during the late Miocene to early Pliocene. The simulated remote responses, including enhanced deep-water formation in the subpolar North Pacific, align well with proxy evidence indicating increased ventilation in that region during the same period (Burls et al. 2017). Notably, unlike previously proposed scenarios requiring elevated atmospheric CO_2 or closed ocean gateways (Curtis and Fedorov 2024; Motoi et al. 2005), our simulations show that topographic forcing alone may be sufficient to activate a vigorous PMOC.

Despite its profound impact on the Pacific, the AM uplift appears to exert limited influence on the AMOC. This asymmetry arises primarily from atmospheric moisture redistribution. In response to the AM uplift, anomalous low-level westerlies emerge over the southern tropical Atlantic (Fig. 2a), enhancing moisture convergence over there. This shift leads to increased precipitation and reduced surface salinity across the tropical and South Atlantic (Figs. 2c-d), thereby suppressing the potential for AMOC enhancement.

Finally, we acknowledge several limitations and uncertainties in this study. First, the imposed abrupt uplift scenario is a simplification of the Andes' complex, time-transgressive orogenic history. It is likely that the wave dynamics cannot be observed during gradual evolution. Consequently, while the ultimate oceanic state may be similar, the transient dynamics we identify may be less apparent in nature. Second, like all other coupled models, CESM1.0 has known biases, which could influence the sensitivity of PMOC and AMOC to topographic forcing. Third, our simulations isolate the effect of AM uplift while holding other boundary conditions fixed, whereas in reality, the late Miocene to early Pliocene was also marked by changes in CO_2 concentrations, ocean gateways (e.g., Panama and Indonesia Seaway), and ice sheet evolution. These co-evolving factors could interact with topographic changes in non-linear ways.

Future work should aim to address these limitations by employing models with improved cloud and ocean mixing schemes, testing uplift scenarios with more realistic temporal evolution, and integrating additional boundary characteristic of the Neogene period. It will also be important to

evaluate model outputs against a broader suite of proxy records, particularly those that constrain changes in North Pacific ventilation, SST–SSS patterns, and inter-basin water mass exchange. Such efforts will help refine our understanding of how tectonic processes reshape global climate and overturning circulation over geological timescales.

Acknowledgment: This research is jointly supported by the NSF of China (Nos. 42288101, 42230403, and 41725021) and by the foundation at the Shanghai Frontiers Science Centre of Atmosphere-Ocean Interaction of Fudan University.

Data Availability Statement:

All data used in this study are available upon request

References

Bond, G., H. Heinrich, W. Broecker, L. Labeyrie, J. McManus, J. Andrews, S. Huon, R. Jantschik, S. Clasen, C. Simet, K. Tedesco, M. Klas, G. Bonani, and S. Ivy, 1992: Evidence for massive discharges of icebergs into the North Atlantic ocean during the last glacial period. *Nature*, **360**(6401), 245–249, https://doi.org/10.1038/360245a0.

Burls, N. J., A. V. Fedorov, D. M. Sigman, S. L. Jaccard, R. Tiedemann, and G. H. Haug, 2017: Active Pacific meridional overturning circulation (PMOC) during the warm Pliocene. *Sci. Adv.*, **3**(9), e1700156, https://doi.org/10.1126/sciadv.1700156.

Curtis, P. E., and A. V. Fedorov, 2024: Spontaneous activation of the Pacific meridional overturning circulation (PMOC) in long-term ocean response to greenhouse forcing. *J. Climate*, **37**(5), 1551–1565, https://doi.org/10.1175/JCLI-D-23-0393.1.

Dekens, P. S., A. C. Ravelo, M. D. McCarthy, and C. A. Edwards, 2008: A 5 million year comparison of Mg/Ca and alkenone paleothermometers. *Geochem. Geophys. Geosyst.*, **9**, Q10001, https://doi.org/10.1029/2007GC001931.

Dowsett, H. J., and M. M. Robinson, 2009: Mid-Pliocene equatorial Pacific sea surface temperature reconstruction: A multi-proxy perspective. *Philos. Trans. Roy. Soc. A*, **367**(1886), 109–125, https://doi.org/10.1098/rsta.2008.0206.

Feng, R., and C. J. Poulsen, 2014: Andean elevation control on tropical Pacific climate and ENSO. *Paleoceanography*, **29**(9), 795–809, https://doi.org/10.1002/2014PA002640.

Fu, M., and A. V. Fedorov, 2024: Impacts of an active Pacific meridional overturning circulation on the Pliocene climate and hydrological cycle. *Earth Planet. Sci. Lett.*, **642**, 118878, https://doi.org/10.1016/j.epsl.2024.118878.

Hu, A., G. A. Meehl, W. Han, A. Abe-Ouchi, C. Morrill, Y. Okazaki, and M. O. Chikamoto, 2012: The Pacific-Atlantic seesaw and the Bering Strait. *Geophys. Res. Lett.*, **39**(3), L03702, https://doi.org/10.1029/2011GL050567.

Hurrell, J. W., M. M. Holland, and Coauthors, 2013: The Community Earth System Model: A framework for collaborative research. *Bull. Amer. Meteor. Soc.*, **94**, 1339–1360, https://doi.org/10.1175/BAMS-D-12-00121.1.

Insel, N., C. J. Poulsen, and T. A. Ehlers, 2010: Influence of the Andes Mountains on South American moisture transport, convection, and precipitation. *Climate Dyn.*, **35**(7–8), 1477–1492, https://doi.org/10.1007/s00382-009-0637-1.

Isacks, B. L., 1988: Uplift of the Central Andean Plateau and bending of the Bolivian Orocline. *J. Geophys. Res.*, **93**(B4), 3211–3231, https://doi.org/10.1029/JB093iB04p03211.

Lamb, S., and P. Davis, 2003: Cenozoic climate change as a possible cause for the rise of the Andes. *Nature*, **425**, 792–797, https://doi.org/10.1038/nature02049.

Maffre, P., J.-B. Ladant, Y. Donnadieu, P. Sepulchre, and Y. Goddéris, 2018: The influence of orography on modern ocean circulation. *Climate Dyn.*, **50**(3–4), 1277–1289, https://doi.org/10.1007/s00382-017-3683-0.

Motoi, T., W. Chan, S. Minobe, and H. Sumata, 2005: North Pacific halocline and cold climate induced by Panamanian Gateway closure in a coupled ocean-atmosphere GCM. *Geophys. Res. Lett.*, **32**(10), L10617, https://doi.org/10.1029/2005GL022844.

Novak, J. B., R. P. Caballero-Gill, R. M. Rose, and Coauthors, 2024: Isotopic evidence against North Pacific Deep Water formation during late Pliocene warmth. *Nat. Geosci.*, **17**, 795–802, https://doi.org/10.1038/s41561-024-01500-7.

Okazaki, Y., A. Timmermann, L. Menviel, N. Harada, A. Abe-Ouchi, M. O. Chikamoto, A. Mouchet, and H. Asahi, 2010: Deepwater formation in the North Pacific during the last glacial termination. *Science*, **329**(5988), 200–204, https://doi.org/10.1126/science.1190612.

Ortiz-Jaureguizar, E., and G. A. Cladera, 2006: Paleoenvironmental evolution of southern South America during the Cenozoic. *J. Arid Environ.*, **66**(3), 498–532, https://doi.org/10.1016/j.jaridenv.2006.01.007.

Rae, J. W. B., W. R. Gray, R. C. J. Wills, I. Eisenman, B. Fitzhugh, M. Fotheringham, E. F. M. Littley, P. A. Rafter, R. Rees-Owen, A. Ridgwell, B. Taylor, and A. Burke, 2020: Overturning circulation, nutrient limitation, and warming in the glacial North Pacific. *Sci. Adv.*, **6**(50), eabd1654, https://doi.org/10.1126/sciadv.abd1654.

Rahmstorf, S., 2002: Ocean circulation and climate during the past 120,000 years. *Nature*, **419**(6903), 207–214, https://doi.org/10.1038/nature01090.

Renny, M., M. C. Acosta, and A. N. Sérsic, 2022: Ancient climate changes and Andes uplift, rather than Last Glacial Maximum, affected distribution and genetic diversity patterns of the southernmost mycoheterotrophic plant *Arachnitis uniflora* Phil. (Corsiaceae). *Global Planet. Change*, **208**, 103701, https://doi.org/10.1016/j.gloplacha.2021.103701.

Richter, I., M. F. Stuecker, N. Takahashi, and N. Schneider, 2022: Disentangling the North Pacific Meridional Mode from tropical Pacific variability. *npj Climate Atmos. Sci.*, **5**(1), 94, https://doi.org/10.1038/s41612-022-00317-8.

Saenko, O. A., A. Schmittner, and A. J. Weaver, 2004: The Atlantic–Pacific seesaw. *J. Climate*, **17**, 2033–2038, https://doi.org/10.1175/1520-0442(2004)017<2033:TAS>2.0.CO;2.

Schmittner, A., T. A. M. Silva, K. Fraedrich, E. Kirk, and F. Lunkeit, 2011: Effects of mountains and ice sheets on global ocean circulation. *J. Climate*, **24**(11), 2814–2829, https://doi.org/10.1175/2010JCLI3982.1.

Sepulchre, P., L. C. Sloan, M. Snyder, and J. Fiechter, 2009: Impacts of Andean uplift on the Humboldt Current system: A climate model sensitivity study. *Paleoceanography*, **24**(4), PA4215, https://doi.org/10.1029/2008PA001668.

Sinha, B., A. T. Blaker, J. J.-M. Hirschi, S. Bonham, M. Brand, S. Josey, R. S. Smith, and J. Marotzke, 2012: Mountain ranges favour vigorous Atlantic meridional overturning. *Geophys. Res. Lett.*, **39**(2), L02705, https://doi.org/10.1029/2011GL050485.

Su, B., D. Jiang, R. Zhang, P. Sepulchre, and G. Ramstein, 2018: Difference between the North Atlantic and Pacific meridional overturning circulation in response to the uplift of the Tibetan Plateau. *Climate Past*, **14**(6), 751–762, https://doi.org/10.5194/cp-14-751-2018.

Takahashi, K., and D. S. Battisti, 2007: Processes controlling the mean tropical Pacific precipitation pattern. Part I: The Andes and the eastern Pacific ITCZ. *J. Climate*, **20**(14), 3434–3451, https://doi.org/10.1175/JCLI4198.1.

Tan, N., Z. S. Zhang, Z. T. Guo, C. C. Guo, Z. J. Zhang, Z. L. He, and G. Ramstein, 2022: Recognizing the role of tropical seaways in modulating the Pacific circulation. *Geophys. Res. Lett.*, **49**(19), e2022GL099674, https://doi.org/10.1029/2022GL099674.

Thomas, M. D., A. V. Fedorov, N. J. Burls, and W. Liu, 2021: Oceanic pathways of an active Pacific meridional overturning circulation (PMOC). *Geophys. Res. Lett.*, **48**(10), e2020GL091935, https://doi.org/10.1029/2020GL091935.

Tong, M., H. Yang, R. Jiang, and P. Wu, 2025: Pivotal role of Tibetan Plateau and Antarctic in shaping present-day Atlantic meridional overturning circulation. *J. Climate*, **38**, 2239–2252, https://doi.org/10.1175/JCLI-D-24-0301.1.

Wen, Q., and H. Yang, 2020: Investigating the role of the Tibetan Plateau in the formation of Pacific meridional overturning circulation. *J. Climate*, **33**(9), 3603–3617, https://doi.org/10.1175/JCLI-D-19-0206.1.

Xu, H., Y. Wang, and S.-P. Xie, 2004: Effects of the Andes on eastern Pacific climate: A regional atmospheric model study. *J. Climate*, **17**(3), 589–602, https://doi.org/10.1175/1520-0442(2004)017<0589:EOTAOE>2.0.CO;2.

Xu, W., and J.-E. Lee, 2021: The Andes and the southeast Pacific cold tongue simulation. *J. Climate*, **34**(1), 415–425, https://doi.org/10.1175/JCLI-D-19-0901.1.

Yang, H., R. Jiang, Q. Wen, Y. Liu, G. Wu, and J. Huang, 2024: The role of mountains in shaping the global meridional overturning circulation. *Nat. Commun.*, **15**(1), 2602, https://doi.org/10.1038/s41467-024-46856-x.

Yuan, S., Y. Liu, Y. Hu, J. Mei, J. Han, X. Bao, X. Li, Q. Lin, M. Wei, Z. Li, Z. Yin, K. Man, J. Guo, Y. Liu, Y. Sun, J. Wu, J. Zhang, Q. Wei, J. Yang, and J. Nie, 2024: Controlling factors for the global meridional overturning circulation: A lesson from the Paleozoic. *Sci. Adv.*, **10**(26), eadm7813, https://doi.org/10.1126/sciadv.adm7813